OBSERVATIONS ON THE INFLUENCE OF LAUNCH VIBRATION ON BEARING TORQUE AND LUBRICANT PERFORMANCE

S.D. Lewis[1], S. Söchting[1, 2], E.W. Roberts[1], I. Sherrington[2]

[1]ESTL, AEA Technology Space, Birchwood Technology Park, Risley, Warrington, WA3 6AT, UK
[2] University of Central Lancashire, Preston, PR1 2HE, UK

Phone +44 (0) 1925 252631, Fax +44 (0) 1925 252415,
E-mail: simon.lewis@aeat.co.uk/soechting@gmx.net

ABSTRACT

In mechanisms where bearing offload systems are not used, ball bearings may be subjected to gapping and transient high contact stresses as a result of launch vibration. Despite the fact that such phenomena may cause bearing damage or degrade torque performance and lubricant life, the dynamic behaviour of bearings subjected to typical launch vibration has been little studied.

This paper outlines recent and ongoing studies concerned with improving our understanding of the influence of vibration effects on ball bearings and their lubricant systems.

In addition to outlining the test set-ups used and discussing test methodologies, an algorithm used to evaluate relative bearing ring displacements and deduce ball-raceway contact stresses under vibration is displayed. The paper will also present study results from recent work and ongoing work and their consequences for bearing users.

1. INTRODUCTION

The maximum peak loads on spacecraft bearings occur at the beginning of their service life due to effects of the launch vibration environment. Thereafter, service loads are relatively low. Provided the bearings and lubricants survive launch, then it is very unusual for a bearing to exhibit fatigue in flight. The usual end-of-life in spacecraft bearings is defined by some form of lubricant failure.

Given this it is clearly of interest to understand how exposure to the launch vibration impacts upon bearing and lubricant performance. The main concerns are that bearings might be subjected to high contact stresses which could cause permanent plastic deformation of balls or raceways or lubricant degradation. The consequences of such damage could be increased torque or torque noise and possibly also reduced lubricant durability leading in the limit to a possible premature mechanism failure in flight. High quasi-static stress is not the only concern however. If the launch vibration forces are much higher than the bearing preload, then the bearing may momentarily offload, allowing a gap between ball and raceway to occur. This will greatly change the dynamic behaviour of the system and possibly permit “hammering” damage to the bearing each time the gap is closed. This phenomenon is known as “gapping”.

From a design viewpoint a frequently asked question concerns the level of gapping allowed in a bearing during launch before damage is likely. In the industry there are a number of design “rules of thumb” which suggest that values of 15-20μm or more of predicted gap within a bearing subjected to launch vibration could be allowable. It is clear that such rules are without detailed experimental justification, though they may be based on practical experience that many bearings with insufficient preload to fully prevent gapping have been launched and function acceptably in flight.

On the other hand logic suggests that a preload which is sufficiently high to prevent ANY gapping during launch provides the lowest risk. This latter high preload approach is also frequently taken, but the consequence (until methods to provide a variable preload during flight are available) is that such bearings may provide a higher than necessary parasitic torque throughout the operational life of the unit. Furthermore as the life of some lubricants is contact-stress dependent, the lubricant life itself and therefore the mechanism operational life MAY be shorter than necessary.

In any real mechanism the situation with respect to vibration is complex, for example both the vibration loads and the dynamic behaviour of the surrounding structure are important parameters. Furthermore in frequently used angular contact bearings it is possible that if damage occurs it will be outside the normal running track of the balls on the raceway (due to the increased contact angle at higher load) and therefore may have little or no impact on bearing performance.
Given the large number of variables, AEA Technology Space has recently performed a number of experimental investigations on relatively simple structures aimed at reaching an understanding of the levels of gapping and

ball loads generated within typical ball bearings under simulated launch vibration.

These studies have been carried out in various Phases :

- A study of the ball-raceway contact stress levels required to cause plastic deformation and the ability to detect indentation optically.
- A study using axial ball bearings of the levels of vibration and gapping at which any visually detectable damage occurs on real bearings.
- A study aimed at generating a methodology for monitoring the gapping in real bearings under vibration and estimating the ball-raceway contact stresses occurring.
- An ongoing study which directly measures in-plane bearing ring displacements during vibration and quantifies the changes in in-vacuo bearing torque which results.

In the remainder of this paper, these studies will be outlined and the principal results from them discussed.

2. STATIC BALL-ON-FLAT INDENTATION

Classical Hertzian theory provides a solution for the dimensions of concentrated contacts under load and the parabolic stress field beneath them, for example, between a normally loaded ball and flat or for a bearing between ball and raceway. The theory assumes elastic material properties and smooth surfaces in contact, which are approximately true for precision engineering components and bearings. As real materials are of limited elasticity, the onset of plasticity, which limits the applicability of the theory, is also of considerable interest.

The classical behaviour of materials is summarised below as described by K.L. Johnson[1] and J.F. Archard[2]. Regimes are defined in terms of parameters p_m and p_o which are the mean and peak Hertzian contact stresses respectively in a contact:

i) $\mathbf{p_m < 1.1Y}$ Purely elastic deformation, in which all deformations applied, is recoverable with only a very small energy loss due to hysteresis (Y is the material Yield Strength in uniaxial tension).

ii) $\mathbf{1.1Y < p_m < 3Y}$ Elastic-plastic deformation, in which there is an increasing degree of local plastic deformation. In the elastic-plastic regime, the plastic deformation is constrained by the elasticity of the surrounding material and so remains sub-surface.

iii) $\mathbf{p_m > 3Y}$ A regime in which fully plastic deformation occurs when the degree of plastic deformation cannot any longer be constrained by the elastic surrounds.

From the above plus application of the Tresca criteria for yield it is possible to identify that yield, which occurs sub-surface, is predicted at a mean Hertzian stress, $p_m \sim 0.4\ H_v$ (or in terms of Peak Hertzian stress, $p_o \sim 0.6\ H_v$). Where H_v is the Vickers hardness number of the material. Applying these relationships to the material properties of SAE52100 bearing steel, which has a typical H_v ~7200 Nmm^{-2} then it is calculated that there is an onset of subsurface yield at p_o~4200 MPa.

This figure agrees well with the specification in ISO76 which states that for "good quality bearing steels" a static load rating of 4200MPa (peak Hertz) applies. This is equivalent to a total residual surface indentation of depth 0.0001D (where D is the rolling element diameter) on removal of the bearing load.

The ESA ECSS-E-30-03 standard suggests that a safety factor of 0.25 should be applied against yield stress for all spacecraft mechanisms. This effectively derates the ISO limit from 4200MPa to 3360MPa (and because of the relationship between load and stress, de-rates the static load limit of bearings to 51% of the allowable values for terrestrial applications).

The above de-rating factor permits different maximum Hertzian contact stresses, based on typical hardnesses. For example SAE 52100 is typically of 700-720H_v, AISI440C around 680H_v. In the experimental work carried out below, the measured hardness of raceways (though manufactured from 52100 steel) was 800H_v.

The objective of this phase was to correlate real measurements of residual plastic deformations with theory and identify any limits on detection.

2.1 Test Method

Loads were applied using a manually controlled press with in-line load cell to bearing rings, which were either lubricated by Braycote 601, MoS_2, ion-plated lead or un-lubricated. The loads applied were recorded on a storage oscilloscope such that the peak load could be easily identified.

Lubricant	Actual load	Pred. Contact Dia. (mm)	Meas. Dent Dia. (mm)	Max. Stress (MPa)	Actual pm/Y plate
None	1296	484	579	10940	2.5
Bray-cote 601	1283	484	648	10901	2.5
MoS_2	1277	481	553	10881	2.5
Lead	3298	682	1060	15415	3.54
Lead	1335	488	640	11043	2.53
None[1]	4970	716	711	4028	1.114
None[1]	4250	612	720	4340	0.97

Table 1 Test Results (All Ball Dia. 3.175mm and Material 52100/52100 except [1] 52100/Groove and Ball Dia 1.588mm)

For the “rough” surfaces the back face of thrust bearing rings was used with zero-peak roughness of order 1.5-2.5µm. For the “smooth” surface tests the superfinished ring groove was used which had a zero-peak roughness of around 0.1µm. Typical results are summarised in Table 1.

2.2 Detectability

Though according to the above theories, permanently detectable surface indentation should not have been present below 3Y, our experiments suggest it can be visible with care at stress levels down to 4000MPa. This is in broad agreement with ISO76, but in conflict with the theoretical treatments of Archard and Johnson.

The detectability of an indentation is clearly dependent on the background roughness and reflectivity and also the presence of any lubricant, changes in which may facilitate detection. For un-lubricated or grease lubricated bearings indentations were only made visible with the greatest of care and under idealised lighting conditions.

On “rough” surfaces indentation was only visible above around p_o>~5000-6000MPa (dents of order 300µm dia.).

On “smooth” surfaces (0.1µm 0-Pk), dents were visible at p_o~4000MPa (100µm half width).

2.3 Conclusion

Due to their low shear strength and hardness, solid lubricant coatings show evidence of contact much more clearly than do liquid or un-lubricated bearings. All contacts with solid lubricants showed some witness marking whereas in contrast indentation damage was only optically detectable with great care for un-lubricated or liquid lubricated contacts. Given this it is sometimes difficult to distinguish a dent from a local change in reflectivity, care is needed when inspecting solid-lubricated bearings post-test.

Based on these static tests it can be concluded that if indentation is “easily” visible on liquid lubricated bearings subjected to vibration under test it is likely that the stresses have locally exceeded around 5000MPa. The loads have therefore exceeded 1.6 times the static load capacity or 3.4 times the ECSS allowable load.

3. BEARING PERFORMANCE INVESTIGATION

Following the above simplified experimental work a second phase was carried out in which axial thrust bearings were subjected to different vibration levels to deduce to what extent vibration and gapping influenced measured torque.

3.1 Test set-up

Thrust bearings were chosen as their contact angle does not change with axial load and in this sense they represent a worst case bearing selection. In order to vibrate 6 bearings simultaneously, small thrust bearings of the type B512 were selected.

The test set-up for torque and vibration testing is shown in Figure 1. Each of the 6 bearing housing stations is mounted on a mounting plate manufactured from aluminium. The weights (2.1kg) are secured to the guide rods via a snubber and nut arrangement.

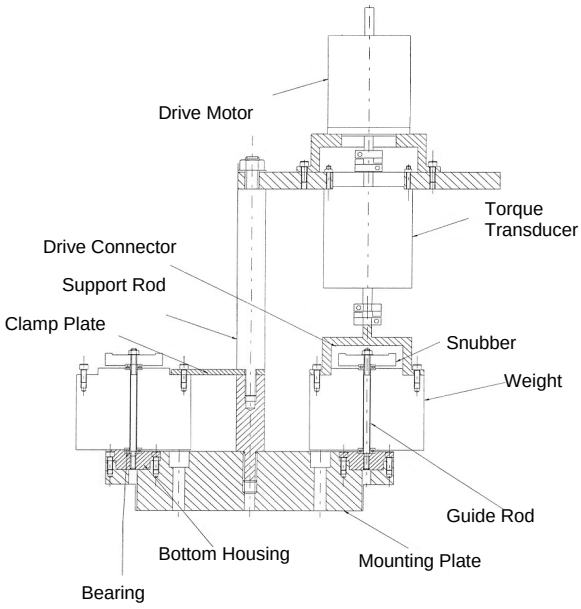

Figure 1 Test set-up for Torque and Vibration Test

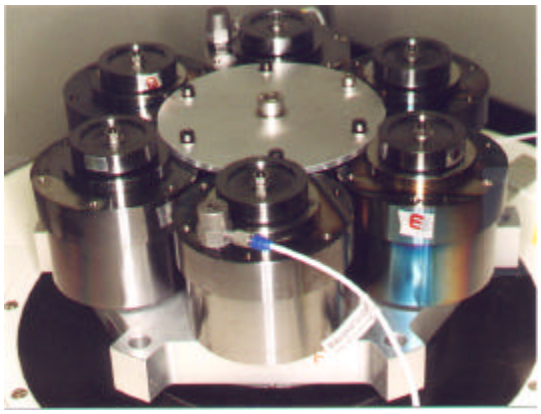

Figure 2 Photograph of Test-set-up

The Torque measurements were carried out in air and in-situ. The drive motor and optical rotary torque transducer were connected in turn to each bearing station, permitting adjustment of preload and measurement of resulting mean torque. Figure 2 shows a photograph of the configuration as tested.

3.2 Test procedure

The lubricants used for the test bearings were Plasmag sputtered MoS_2, ion-plated lead and Braycote 601 grease. The "slave" bearings were lubricated with Pennzane SHFX2000 oil.

To prevent motion during vibration, both bearing seats and fasteners were secured with a Loctite compound. The preload was set by adjustment of the locking screw such that the mean torque of the bearings was in the range 75gcm ± 10%. This was calculated to give a preload equivalent to 328 N ± 7% preload.

The stiffness of the assembly was essentially controlled by the stiffness of the central guide rod plus the non-linear stiffness of the bearing balls. The guide-rod stiffness was of order 6 10^7 N/m and the first frequency of the test structure was calculated at 400Hz, thus to avoid complications from substantial dynamic effects tests were mainly carried out at 4g and 8g input acceleration levels and 300Hz, though in some cases the amplitude was increased.

Input and response accelerations were measured on the baseplate and on the test mass itself (in orthogonal planes such that axial and radial motions could be monitored). The tests were confined to sinusoidal vibration inputs to facilitate understanding of input and response levels.

3.3 Results

Taking results from more than 20 tests together no real correlation was experienced between change in bearing torque and gapping as illustrated in Figure 3. For example the two largest changes in bearing torque were experienced with no gapping and 18 µm gapping respectively. Considering only those 3 tests carried out which resulted in stresses below the ECSS limit for the material, then a trend was apparent of increasing gapping and torque noise ratio.

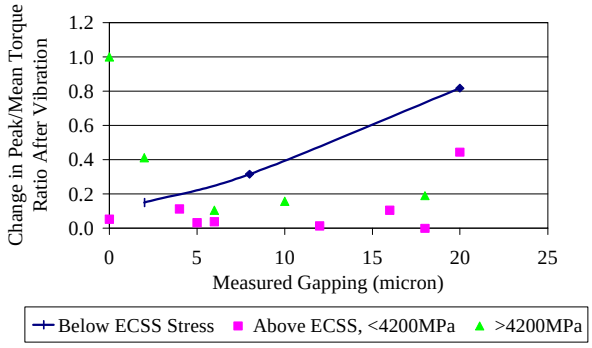

Figure 3 Changes in Torque noise from gapping

3.4 Conclusions

Despite the fact that the measured accelerations and forces generated during vibration were mostly insufficient to cause permanent indentation damage, there was always an increase in bearing torque noise (measured as peak-mean torque value) post-test. Typically bearings showed an increase of 24% in peak-mean torque values over their pre-test values and in some cases up to 100%. There was no observable difference in the performance of the different lubricants in air or on the performance of the non-lubricated bearings in this respect.

Solid lubricated bearings subjected to vibration tests typically also showed some local degradation of the lubricant films in the vibration affected zones. Though from this test campaign it was not possible to state to what extent this damage affected the in-vacuo lubricant film durability or effectiveness (this is to be assessed in the present campaign). Experience suggests that such features may well "repair" with extended running.

4. GAPPING TEST METHODOLOGY

Subsequent to the above observations a third test phase was executed in order to permit fundamental studies into the ring motions in more flight-representative, angular contact bearings.

Unfortunately it was not possible to identify direct displacement measurement devices which could provide a multi-channel capability for measurements in axial, radial and tilt directions with micron precision at reasonable cost. Therefore a technique was identified which permitted derivation of ring displacement data from miniature triaxial accelerometers mounted directly onto the inner and outer bearing rings. The algorithm used is described below.

4.1 Algorithm Verification and Generation

Using the assumption that bearing rings move as rigid bodies under vibration force, use of 3 triaxial accelerometer mounted directly onto the inner and outer rings (18 data channels) permits ring motion to be determined under 6-degree of freedom.

The relative displacements of the bearing rings are calculated by double integration of accelerations. The double integration of the acceleration-time record is carried out by numerical integration.

The time domain acceleration vector $a(t)$ can be Fourier transformed as:

$$a(t) \Leftrightarrow A(jw)$$

Then the velocity $v(t)$ and displacement $s(t)$ transforms as:

$$v(t) \Leftrightarrow A(jw)/jw \qquad s(t) \Leftrightarrow A(jw)/-w^2$$

The above algorithm was coded into LabVIEW and validated by experiments in which the calculated displacement data from a single axis accelerometer was

compared with directly measured displacement data from a single axis fibre optical displacement transducer. Similar data from the Data Physics control software used to control the shaker was also examined, this too calculates displacement from acceleration using a double integration method. The test set up is shown in Figure 4 and the results are summarised in Table 2 below.

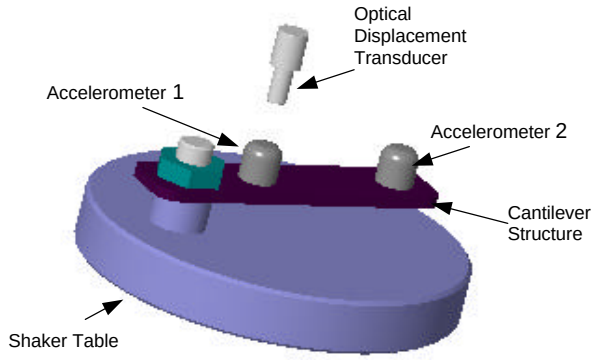

Figure 4 Test set-up for Verification of Displacement Measurement

	Data Physics Controller		LabVIEW software		Displacement probe
	Acceleration (g)	Displacement (microns)	Acceleration (g)	Displacement (microns)	Displacement (microns)
Acc1	3.00	92.06	3.00	92.04	94.00
Acc2	1.47	45.19	1.47	45.19	44.60

Table 2 Comparison of Displacements measured for a 3g Sine Wave

Though this methodology was verified numerically, when real signals were used, close agreement was only found at the beginning and the end of the calculated time domain displacement solution. In the central portion, values were clearly incorrect as a "necking" reduction in signal amplitude was observed. This error was attributed to leakage in the FFT routine. It did not occur if the frequency of the signal was an even multiple of the sampling resolution.

By using only the first 10% of double integrated time domain displacement data, displacement agreement within 3% of the experimental value was found. In this way the leakage problem was avoided.

The final stage in the algorithm development was to verify the method applied to multiple points on the assumed rigid rings such that the relative linear displacements and tilt vectors from the double integrated acceleration data could be evaluated.

The algorithm generation assuming displacements are measured at 3 points on inner and outer rings as shown in Figure 5 is shown below. If displacements at accelerometer locations 1,2,and 3 are x_1, y_1, z_1; x_2, y_2, z_2 and x_3, y_3, z_3; the translations at the ring centre are X, Y, Z and the small tilts about X, Y and Z are θ_1, θ_2, θ_3 then:

$x_1 = X - r\,\theta_3$ $\quad x_2 = X$ $\quad x_3 = X$

$y_1 = Y$ $\quad y_2 = Y + r\,\theta_3$ $\quad y_3 = Y = Y - r\,\theta_3$

$z_1 = Z + r\,\theta_1$ $\quad z_2 = Z + r\,\theta_2$ $\quad z_3 = Z = Z + r\,\theta_2$

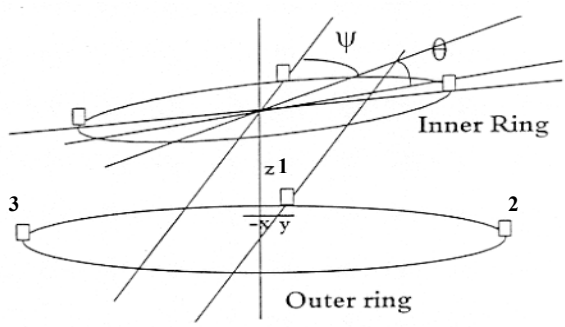

Figure 5 Schematic of Relative Ring Displacement

The resulting tilt angle is,

$$\theta^2 = \theta_1^2 + \theta_3^2,$$

the angle of the tilt axis to the Y axis is

$$\Psi = \tan^{-1}(\theta_2/\theta_1).$$

The solution of this algorithm was also coded in LabVIEW.

The final phase of the analysis was to generate data on bearing peak Hertzian contact stress for measured axial, radial and angular displacements of the rings given the experimental preload compliance. This data was generated using individual quasi-static analyses within CABARET, though it would be possible to use the CABARET code to generate regression surfaces if there were a requirement to directly predict stresses on-line during a test.

Following development of the algorithm, tests were carried out to measure the ring motion and gapping on SEA65 angular contact bearings.

4.2 Gapping Test Set up

The accelerations are measured using miniature triaxial accelerometers (Kistler8694M1), attached to the bearing rings (Figure 5). The accelerometers have a mass of 2.5g and a 5mm square footprint for adhesive mounting onto the edge of the bearing rings.

The data logging system had a 19 channel signal conditioning and processing capability, comprising 18 channels for the accelerometers on the rings plus one for the shaker control.

The general arrangement of the test set-up is shown in Figure 6. The mechanical system comprises a single central stub shaft with a test bearing pair housed within an outer housing and located by clamp rings.

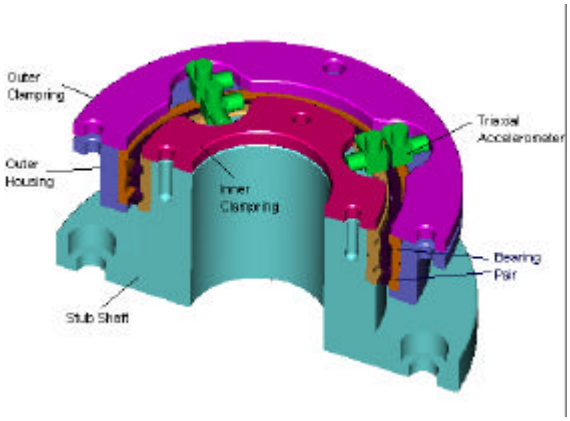

Figure 6 General Arrangement of Test set-up

The test bearings used are matched face to face pairs of angular contact ball bearings (SNFA SEA65 7CE1 FFL) selected for their large diameter and because their 3mm ring width is adequate for accelerometer mounting and as a target for the non-contacting displacement transducer. The details of the used bearings are shown in Table 3.

SNFA SEA 65 7 CE 1 FFL	
Bore(mm)	65
Outer Dia.(mm)	85
Bearing with (mm)	10
Ball Complement	29
Test Ball Complement	5
Contact Angle (°)	15
Preload (N)	71
Conformity No (Inner Race and outer race)	1.04
Ball Dia.(mm)	5.555

Table 3 Geometry of Bearings used in Gapping Study

A further consideration was that because of their large size, the ring mass is 51 grams, the additional mass of the accelerometers could be expected to have only small impact on their behaviour. The three accelerometers comprise therefore only an additional 15% of total ring mass or 1% of the total moving mass of the outer housing assembly. The face-to-face bearing orientation was chosen because it differs from the back-to-back pair by giving lower rigidity to the assembly and therefore having lesser ability of withstanding tilting moments.

The nominal preload of the matched pair is set by the bearing offset. However in order to get large gaps for modest accelerations it was necessary to reduce the ball complement. Using CABARET v 1.09 it was calculated that for the reduced ball complement used in the test (5 balls) the nominal preload was 11.3N based on the nominal offset.

4.3 Gapping Test Procedure

Immediately before and after each test a low level sine sweep from 30-2000 Hz with 0.5g acceleration was carried out. During this sweep the z-axis vibration levels on the base, inner and outer rings were monitored. One objective of the sine sweep was to characterise the low-level response of the system prior to shaking. The other was to permit comparison with post-test behaviour to ensure no significant changes had taken place.

On completion of the initial sine sweep a series of increasing sinusoidal dwell tests were carried out. In these tests a set amplitude and frequency of sinusoidal acceleration was maintained for a period of 2 minutes or until all data was recorded. In each case the input acceleration was at 300 Hz and the responses were monitored at this frequency on the controller. During each dwell test, all 19 channels of acceleration data were logged by sampling 8192 samples at 8192 Hz.

Data processing to permit derivation of ring motions and predicted peak Hertzian stresses was carried out off-line after the test. The Test matrix and the applied accelerations are summarised in Table 4.

Test I.D.	Vibration level	Nominal Acceleration (g)	Preload Spring Stiffness (N/m)	Pre-load (N)
1	Low	4	3.00E+05	98
2	High	20	3.00E+05	98
3	Low	4	3.20E+06	11
4	High	20	3.20E+06	11
5	Low	4	6.00E+08	11
6	High	20	6.00E+08	11
7	Low	4	2.00E+07	11
8	High	20	2.00E+07	11
9	Low	4	3.00E+05	11
10	High	20	3.00E+05	11
11	Random Low	4grms (12g peak)	2.00E+07	11
7a	V. High	50	6.00E+08	11
6a	V. High	50	2.00E+07	11

Table 4 Gapping Test Matrix

To permit some modification of the preload stiffness, springs were applied in the load line.
Finally measured gapping was compared to that predicted using the quasi-static loading and CABARET analysis.

5. RESULTS AND DISCUSSION

The effects of vibration on the bearings were assessed in a number of ways.

- All bearings were torque tested by carrying out a few revs pre- and post-test at low speed in air. From these tests measurement of mean and zero-peak values were made to permit comparison.
- All bearings were subjected to examination under a low power optical microscope, and those with the more interesting features were subsequently subjected to energy dispersive X-ray (EDAX) analysis and optical profilometry.

From the torque noise measurements made, there seems little correlation between maximum bearing gapping or maximum acceleration and increases in bearing torque noise.

During the optical examination it was notable that the greased and un-lubricated bearings showed very slight surface damage whereas the witness of vibration was much more noticeable for the solid lubricated bearings due to changes in reflectivity.

In some cases, following vibration, localised degradation of solid lubricant films was observed. For example, in one case where a bearing was exposed to a combination of high stress and gapping, the ion-plated lead film was almost completely removed locally. The bearing in question was exposed to an acceleration of 5g and assuming equal load sharing between balls a peak Hertzian stress of 4105Mpa (25% higher stress and 100% higher load than allowed under ECSS standard.), and 5.5 μm maximum gapping.

Figure 7 below shows a Scanning Electron Micrograph (SEM) of the vibration-affected zone of the inner raceway. The central wear band from pre- and post-test torque measurements and a number of small elliptical vibration affected zones can be seen. Figure 8 shows the surface of the main elliptical zone at its intersection with the wear track and the non- vibration affected zone.

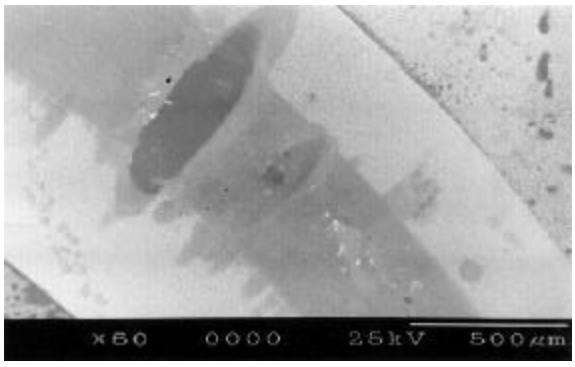

Figure 7 Scanning Electron Micrograph of Lead lubricated Raceway post-test

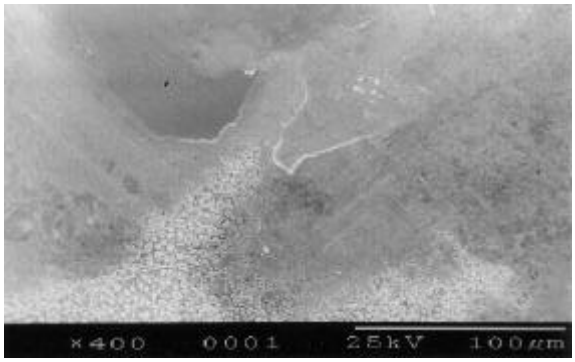

Figure 8 Scanning Electron Micrograph of the Edge of elliptical Zone of Lead lubricated Raceway shown in Figure 7

An EDAX examination of the raceway in Figure 7 shows that the Pb-peak detected in the non-vibration-affected zone, described by figure 9, is similar to the Pb-peak detected in ball track.

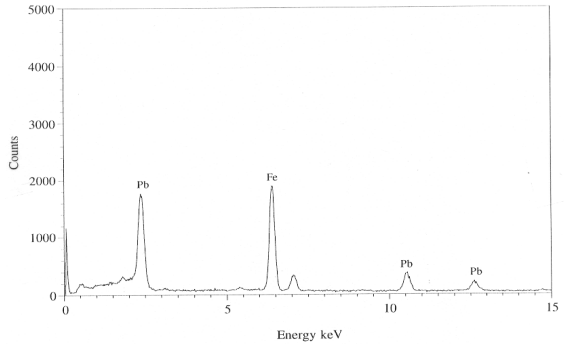

Figure 9 Energy Disperse X-ray Profile of Raceway of Figure 7 Non-Vibration-affected Zone

However the Pb-peak in the vibration-affected zone is hardly detectable as figure 10 shows.

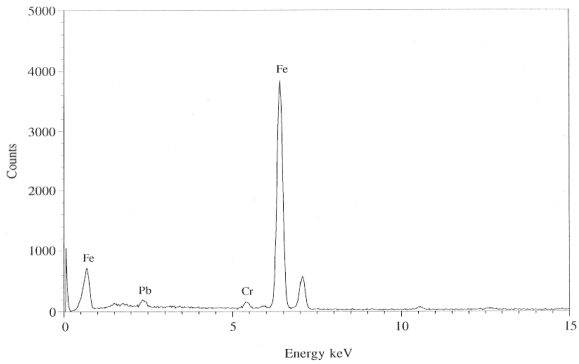

Figure 10 Energy Disperse X-ray Profile of Raceway of Figure 7 Vibration-affected Zone

No evidence of similar damage to the lead lubricant was found at lower levels of stress with any other bearings during this programme.

In the case of MoS_2 lubricated bearings the vibration-affected zones were much more difficult to identify and showed also less reduction of the lubricant film in the EDAX analysis.

The damage to the grease lubricated bearings was much less. Even after removing the grease with solvent the vibration-affected zones were barely detectable against the background raceway curvature.

The bearing performance investigation assumes that the vibration load is shared equally between all balls of the bearing. Where gapping occurs the entire vibration load might be instantaneously passed through a single ball/raceway contact. Therefore the load-bearing assumption may not be true, however it is not possible to verify to what extent the load has been borne by a reduced ball complement, without the measuring of loads at individual contacts.

The results of this gapping investigation are summarised in Table 5. It shows that though measured axial ring displacements are in the range of 1-25 microns and parasitic radial accelerations are only of order 5-10% of the axial input, radial deflections are of the same order. However tilt angles are very small, suggesting rings remain substantially parallel and that therefore ball loads may in fact be distributed uniformly as assumed above.

The CABARET-predicted and measured gapping values were found to be in good agreement, typically errors observed in gapping predictions are of order 20-30% and in derived stress predictions only 10%. However measured radial ring motions and tilt are not entirely consistent with predictions, perhaps because the radial motions are "free-flight" motions not constrained by bearing geometry (and thus not modelled in CABARET).

I.D	Peak sine	Axial Displacement (mm)		Radial Displacement (mm)		Resultant tilt ($°x10^{-6}$)	
	Acc.(g)	RMS	Max	RMS	Max	RMS	Max
1	4	2.9	7.9	4.9	10.0	11.9	25.2
1	4	1.9	5.8	4.1	8.4	6.2	16.6
1	4	2.4	6.6	4.5	10.8	6.5	15.3
1	4	2.9	7.4	6.7	15.4	5.8	11.7
2	20	14.1	35.3	8.6	21.9	14.2	36.0
3	4	3.0	8.0	5.5	12.0	9.9	20.2
4	20	10.8	19.7	8.4	15.9	16.2	39.1
5	4	2.6	5.2	4.3	9.9	7.3	14.3
6	20	7.3	13.0	5.4	12.2	12.0	32.4
7	4	2.5	5.7	4.4	9.4	5.8	14.7
8	20	5.6	13.7	5.5	12.5	9.7	21.3
9	4	2.9	7.4	6.7	15.4	5.8	11.7
10	20	8.3	16.1	7.4	19.6	12.9	30.7
11	4	3.4	11.3	5.1	12.2	9.5	20.6
7a	50	24.1	53.2	19.2	35.4	21.5	50.2
6a	50	22.6	46.1	10.4	25.4	40.8	98.2

Table 5 Summary of Gapping-Test Results

6. CURRENT INVESTIGATION

The technique above can provide a useful understanding of sinusoidal vibration however it cannot be adapted for use in random vibration monitoring due to the errors, which are attributed to leakage in the FFT analyses.

Clearly an understanding of the effects of random vibration both on the bearings and the lubricants themselves is the ultimate aim.

An ongoing programme of work is underway which will use direct non-contacting displacement transducers to monitor axial and radial ring motions. These devices are able to measure direct and non-intrusively the displacement of the bearing rings, without the errors associated with the accelerometer method.

The planned test campaign involves both solid and liquid lubricated bearings. In accordance with typical flight practice, the solid lubricated bearing pairs are lubricated with ion-plated lead on raceways with a leaded bronze cage and the liquid lubricated bearing pairs are lubricated with Braycote 601EF grease on raceway with a Fomblin Z25-impregnated phenolic cage.

In a simulation of flight practice, the bearing torque will be characterised by measurement of mean and peak torque followed by exposure to vibration in-air and immediate re-characterisation in-vacuo. This procedure will be repeated with varying levels of accleration until post-test torque exceeds some threshold.

7. CONCLUSION

This programme of work has been a first step toward a greater understanding of a complex problem with real implications for design engineers.

The main conclusions of the study so far are:

1) Evidence of vibration is much more clearly defined in the case of solid lubricated bearings due to changes in reflectivity.
2) There seems little correlation so far between gapping, contact stress and changes in bearing torque. The gapping "rules of thumb" have not so far been substantiated. Increases in torque noise should be expected after all vibration tests.
3) It has not been possible to state to what extent any visible damage affects lubricant film durability or effectiveness in vacuum, nor if such damage may repair with extended running.

The ongoing work is expected to provide some indications about the extent to which bearing torque is affected by damage to solid films and to what extent they are capable of self-repair.

8. REFERENCES

1. Johnson, K.L. 1985, Contact Mechanics, Cambridge University Press

2. Archard, J.F., Wear Control Handbook

3. Lewis, S.D. 1998, Effects of Launch Vibration on Ball Bearings ESTL/TM/216

4. Lewis, S.D. 1999, Ball bearing Vibration-Induced Gapping Study ESTL/TM/232